Frontiers of Information Technology & Electronic Engineering
www.jzus.zju.edu.cn; engineering.cae.cn; www.springerlink.com
ISSN 2095-9184 (print); ISSN 2095-9230 (online)
E-mail: jzus@zju.edu.cn

Trajectory optimization with constraints for alpine skiers based on multi-phase nonlinear optimal control*

Cong-ying CAI, Xiao-lan YAO†‡

School of Automation, Beijing Institute of Technology, Beijing 100081, China

†E-mail: yaoxiaolan@bit.edu.cn

Received Oct. 30, 2019; Revision accepted Feb. 21, 2020; Crosschecked Aug. 28, 2020

Abstract: The super giant slalom (Super-G) is a speed event in alpine skiing, in which the skier trajectory has a significant influence on the athletes' performances. It is a challenging task to determine an optimal trajectory for the skiers along the entire course because of the complexity and difficulty in the convergence of the optimization model. In this study, a trajectory optimization model for alpine skiers competing in the Super-G is established based on the optimal control theory, in which the objective is to minimize the runtime between the starting point and the finish line. The original trajectory optimization problem is converted into a multi-phase nonlinear optimal control problem solved with a pseudospectral method, and the trajectory parameters are optimized to discover the time-optimal trajectory. Using numerical solution carried out by the MATLAB optimization toolbox, the optimal trajectory is obtained under several equality and inequality constraints. Simulation results reveal the effectiveness and rationality of the trajectory optimization model. A test is carried out to show that our code works properly. In addition, several practical proposals are provided to help alpine skiers improve their training and skiing performance.

Key words: Trajectory optimization; Optimal control; Pseudospectral method; Optimal trajectory; Numerical solution
https://doi.org/10.1631/FITEE.1900586 **CLC number:** O232; TP29

1 Introduction

The super giant slalom (Super-G) is a compulsory racing discipline in alpine skiing at the International Ski Federation (FIS) Alpine World Ski Championships, FIS Alpine Ski World Cup, and Olympic Winter Games. This sport combines speed and skill perfectly. Some skiers tend to focus on speed and neglect the skier trajectory so that they cannot obtain an optimal rank. In recent years, alpine skiing has become popular in sports studies. However, few achievements have been realized in optimal trajectory in alpine skiing. For alpine skiers, skiing ability is the most basic skill, and the skier trajectory is also crucial, because it reflects not only the skiing skills of the skier, but also the significant role the trajectory plays in medal competitions. In other words, a time-saving skier trajectory is tremendously important for alpine skiers to improve performance. Therefore, establishment and analysis of a trajectory optimization model have practical significance.

There are many research works into the trajectory optimization in alpine skiing. In these studies, there are mainly three types of modeling methods, i.e., particle model, ski model, and rod model.

The ski-skier system was treated as a particle in Sundström et al. (2011) and Dębski (2014). This model is relatively simple and effective. Considering the influence of different forces, dynamic equations are established in each component force direction, but some factors are often ignored, such as snow cutting force, thrust of ski poles, geometric features of skis, and postural angles of the human body. Because of the

‡ Corresponding author

* Project supported by the Key Technology Research and Demonstration of National Scientific Training Base Construction of China (No. 2018YFF0300800)

ORCID: Xiao-lan YAO, https://orcid.org/0000-0002-7699-8634

appropriate simplification of the whole ski-skier system, the model has obvious advantages in numerical solution and convergence.

The ski-skier system was treated as a ski model in Hirano (2006), in which the quickest descent line between gates on a ski slope was calculated. In the model, some details were considered, such as positions of the ski-skier system on the ski slope, rotational angles of the skis, ski length, ski slope angle, system velocity, and rotational velocity at a discrete time. However, simulation results seem to be unsatisfactory. The quickest descent line through four gates could not be obtained due to the numerical difficulty. Instead, the descent lines are calculated separately for uphill and downhill turns, and then they are simply added. A ski model was established by Chen L and Qi (2006). In their work, based on the geometric characteristics of skis and the formula for turning radius, constraint equations for ski turning movement were deduced using a numerical method, and numerical simulations and analysis of the ski movement trajectories on flat ground and a slope were carried out, including the trajectory of the body's center of gravity and the trajectory of the geometric center of the ski.

Furthermore, the ski-skier system can be treated as a rod model, which is a slightly complicated rod system. In the modeling process, the skier's body is simplified as a massless rod and a mass point, and the mass point is affixed to the upper end of the rod. By building a rod model, a skier's movement was analyzed (Youn, 2018), the dynamics of the carving runs in alpine skiing was studied (Komissarov, 2019), and the effect of the skier's inclination during the turning motion around the pole on the total descent time was considered (Rudakov et al., 2010). Nevertheless, it is difficult to solve a trajectory optimization problem based on the rod model and obtain an optimization result for an alpine skiing course with multiple gates.

To address the trajectory optimization problem, some methods have been proposed. For instance, numerical methods for trajectory optimization were summarized in detail (Betts, 1998; Chen G et al., 2011; Huang et al., 2012; Rao, 2014), including mainly two categories: direct and indirect methods. A hybrid approach, a combination of direct and indirect methods, was described as a promising way to obtain a numerical solution to nonlinear optimal control problems (von Stryk and Bulirsch, 1992). A dimension reduction method based on trajectory shaping was put forward to improve the accuracy of trajectory optimization using the good shape-characterizing ability of Bézier curves to describe the optimal trajectory, and the dimension reduction optimization method converts the boundary conditions of the optimization problem into the parameter constraints of trajectory shaping (Zhang and Hou, 2016). An in-cruise optimization method was implemented to calculate the optimal trajectory that reduces the flight cost, by which the aircraft could perform a horizontal deviation or change altitudes via step climbs to reduce fuel consumption (Patrón and Botez, 2015).

Some recent works have thoroughly considered the trajectory optimization problem. A joint trajectory smoothing and tracking framework for a specific class of targets with smooth motion (Li et al., 2019) was presented; it models the target trajectory over a time window by a continuous function of time (FoT) and updates the parameters iteratively with the time sliding of the time window. Based on the recursive Bayesian filtering and the least squares fitting (LSF) frameworks, a computationally efficient approach to exploiting the prior trajectory geometry (Li, 2019) was presented, for positioning a target that moves on a single, deterministic road. An improved dynamic programming track-before-detect (DP-TBD) algorithm was proposed (Zheng et al., 2016) to distinguish the target from the disturbance more effectively, and the improved algorithm does not need prior knowledge about the target motion. An adaptive multi-spline refinement algorithm, a new dynamic programming based parallel algorithm, adapted to on-board heterogeneous computers was studied by Dębski (2016); it uses a new discrete space of C^1-continuous functions called the multi-spline as its search space representation. Guo et al. (2019) proposed an efficient dynamic programming with shooting heuristic as a subroutine (DP-SH) algorithm for the integrated optimization problem. Chen D et al. (2019) proposed a multi-objective trajectory planning method based on an improved immune clonal selection algorithm to plan the motion trajectory of the mobile platform in the Cartesian space with a quintic B-spline curve. Liu et al. (2019) proposed a stochastic optimal control algorithm to dynamically adjust and optimize aircraft trajectories. A novel guidance algorithm based on convex optimization, pseudospectral

discretization, and a model predictive control (MPC) framework was proposed by Wang et al. (2019) to solve the highly nonlinear and constrained fuel-optimal rocket landing problem. These algorithms have different applications in the field of trajectory optimization, and play an important role in trajectory optimization.

In addition, several kinds of software are used for trajectory optimization, especially in aircraft, such as GPOPS (Graham and Rao, 2015; Benito and Johnson, 2016; Hong et al., 2016), SEPSPOT, OTIS (Falck and Gray, 2019), POST, CAMTOS, VITA, CHEBYTOP (Paek et al., 2016), and TOMLAB (Morbidi et al., 2018; Ranogajec et al., 2018; Crain and Ulrich, 2019).

Although some achievements have been made in the research on alpine skiing, it is worthwhile to study and analyze the trajectory optimization model in depth. Therefore, we are eager to do some work in this area.

The main contributions of our study are summarized as follows:

1. We build a trajectory optimization model. On one hand, comparing it with other current methods for establishing dynamic equations, we derive a set of simpler dynamic equations, and find that the proposed method is easier to converge (i.e., obtain the optimal solution for an alpine course with multiple gates). On the other hand, in the modeling process, we choose the Super-G course as the research object and take the course data from the official website of FIS, so the course setting is within reason.

2. Gliding inflection points are marked on the optimal skier trajectory. These points are the transition points for concavity and convexity in the ski trajectory; however, they have not been presented in the optimal ski trajectory in other works in terms of concept and coordinate labeling.

3. Several practical proposals are put forward after analysis. It is hoped that these reasonable suggestions can help in the daily training and provide efforts for performance improvements for alpine skiers.

2 Course setting

To make our research object concrete and representative, a Super-G course is chosen. Alpine skiing is divided mainly into two types: the speed events (Downhill and Super-G) and technical events (Slalom and Giant Slalom). In Downhill, Super-G, and Giant Slalom, two pairs of slalom poles are used, each pair of which carries a gate panel between them. There are single-color gates in Downhill, and the Giant Slalom and Super-G alternate red and blue gates. Although the gate color settings are different, they have no influence on the research. The biggest difference is in the requirements for the gate intervals and the vertical drop of the whole course. The choice of the Super-G is mainly due to that it is a concrete and representative research object for the three events.

To build a more efficient and effective trajectory optimization model for alpine skiers in the Super-G, the Super-G course is designed according to technical data taken from the International Competition Rules (ICR) on the fis-ski.com webpage (https://www.fis-ski.com/en/inside-fis/document-library/alpine-documents), whereby only seven Super-G gates are arranged for the study. In Fig. 1, a Super-G gate consists of four slalom poles and two gate panels, where the gate line is the shortest imaginary line between the turning pole and the outside gate at snow level. By establishing a Cartesian coordinate system, whose x and y axes are parallel to the horizontal and longitudinal directions, respectively, of the ski slope, the coordinate positions of the starting point, inside poles, and the finish line can be determined. Ski slope is assumed to have an angle β and a flat surface. The two inside poles of each gate are marked, and the coordinates of which (unit: m) are shown in Fig. 2.

Many different trajectories can remain after athletes run the ski course several times. However, an admissible trajectory demands that the skiers pass the

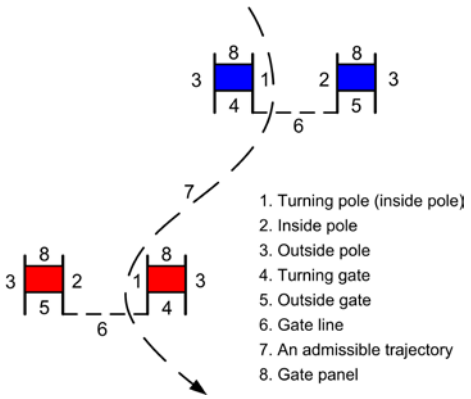

Fig. 1 Super-G gate components

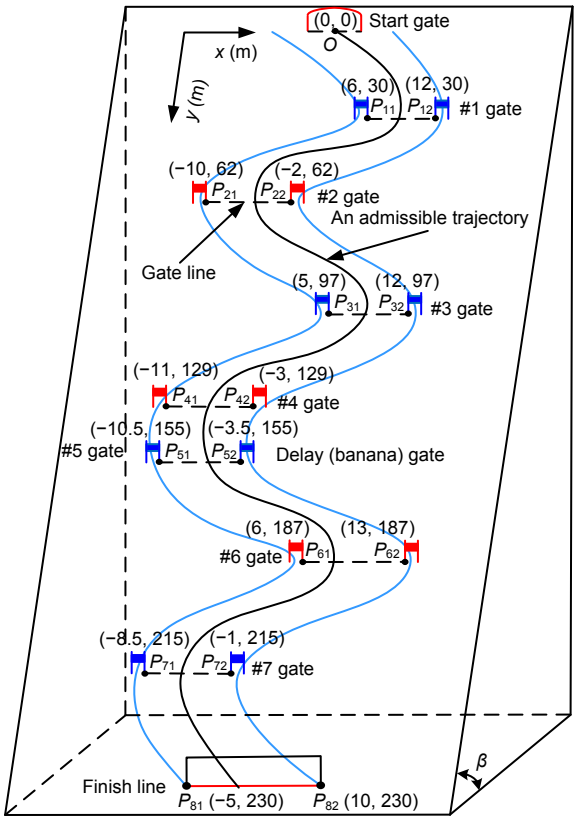

Fig. 2 An alpine skiing course for the Super-G

gate lines between two inside poles such that the skiers' ski tips and two feet have crossed the gate line, in contrast to the wrong way of bypassing the outside poles. If a competitor misses a gate, he/she can no longer go through further gates and will eventually fail in the race. Therefore, the coordinate positions of the inside poles can be transformed into the boundary conditions for the trajectory optimization model.

3 Modeling and solution

3.1 Particle model

As mentioned above, considering the complexity and convergence of the trajectory optimization model, the whole ski-skier system, including the human body and two ski poles and skis, is regarded as a particle, whose mass is m. Assume that the particle glides along an admissible trajectory and all turns are purely carved (i.e., without skidding or take-off). Ski poles are not used to change the direction of the skier's gliding and the magnitude of the skier's velocity. Only five forces acting on the particle are described, i.e., gravity G, supporting force F_N, sliding friction f_s, air resistance (air drag) f_a, and resultant force F_c which provides centripetal force in the radial direction (Fig. 3). Note that F_N is perpendicular to the slope and that all the other forces are on the slope. Moreover, v and $\dot{\varphi}$ denote the instantaneous speed and angular velocity at a certain moment, respectively (Fig. 3b).

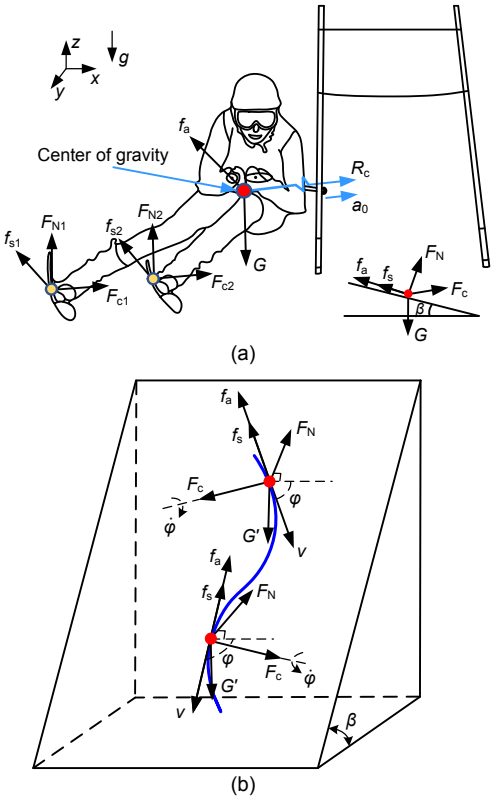

Fig. 3 Forces acting on an alpine skier: (a) component forces generated at each point of action; (b) forces applied to a particle on an admissible trajectory

3.2 Deriving equations

On the ski slope, we perform force analysis on the particle model (Fig. 4). After applying Newton's Second Law in the x_1 and y_1 directions, we can obtain

$$\begin{cases} m\ddot{x}_1 = -F_c\sin\varphi - (f_a + f_s)\cos\varphi, \\ m\ddot{y}_1 = G' + F_c\cos\varphi - (f_a + f_s)\sin\varphi, \end{cases} \tag{1}$$

where

$$\begin{cases} G' = mg\sin\beta, \\ f_a = 0.5C_d\rho_a s v^2, \\ f_s = \mu mg\cos\beta, \end{cases} \tag{2}$$

where μ is the sliding friction coefficient, C_d the air resistance coefficient, ρ_a the air density, and s the windward area of the human body. In the same way, in the x_2 and y_2 directions, we can obtain

$$\begin{cases} m\ddot{x}_2 = F_c\sin\varphi - (f_a + f_s)\cos\varphi, \\ m\ddot{y}_2 = G' - F_c\cos\varphi - (f_a + f_s)\sin\varphi. \end{cases} \tag{3}$$

Considering that $\dot{\varphi} > 0$ (because φ increases over time) on the upper half part of the trajectory and $\dot{\varphi} < 0$ (because φ decreases over time) on the lower half part of the trajectory, we can obtain the general expression as

$$\begin{cases} m\ddot{x} = -F_c\sin\varphi\operatorname{sgn}\dot{\varphi} - (f_a + f_s)\cos\varphi, \\ m\ddot{y} = G' + F_c\cos\varphi\operatorname{sgn}\dot{\varphi} - (f_a + f_s)\sin\varphi. \end{cases} \tag{4}$$

We do not want to obtain the overly complex dynamic equations used for trajectory optimization. Therefore, we attempt to cancel out F_c. According to the kinematic knowledge of

$$\begin{cases} \ddot{y} = (v\sin\varphi)' = \dot{v}\sin\varphi + v\dot{\varphi}\cos\varphi, \\ \ddot{x} = (v\cos\varphi)' = \dot{v}\cos\varphi - v\dot{\varphi}\sin\varphi, \end{cases} \tag{5}$$

and combining Eqs. (4) and (5), the following equation holds:

$$\begin{aligned} & m\ddot{y}\cos\varphi - m\ddot{x}\sin\varphi = G'\cos\varphi + F_c\operatorname{sgn}\dot{\varphi} \\ \Rightarrow\ & m(\dot{v}\sin\varphi + v\dot{\varphi}\cos\varphi)\cos\varphi - m(\dot{v}\cos\varphi - v\dot{\varphi}\sin\varphi)\sin\varphi \\ & = G'\cos\varphi + F_c\operatorname{sgn}\dot{\varphi}. \end{aligned}$$

For simplification, we can obtain

$$mv\dot{\varphi} = G'\cos\varphi + F_c\operatorname{sgn}\dot{\varphi}. \tag{6}$$

Appling Newton's Second Law in the radial and tangential directions, we can obtain

$$\begin{cases} m\dot{v} = G'\sin\varphi - (f_a + f_s), \\ F_c + G'\cos\varphi\operatorname{sgn}\dot{\varphi} = mv^2/R_c, \end{cases} \tag{7}$$

where R_c is the turning radius (i.e., the radius of curvature) that reflects the bending degree of the skier trajectory at a certain point. Combining Eq. (6) and the second equation of Eq. (7), the following equation holds:

$$\dot{\varphi} = \frac{v}{R_c}\operatorname{sgn}\dot{\varphi}. \tag{8}$$

Consequently, we can obtain

$$\begin{cases} \dot{\varphi} = \dfrac{v}{R_c}\operatorname{sgn}\dot{\varphi}, \\ \dot{v} = \dfrac{G'\sin\varphi - (f_a + f_s)}{m}. \end{cases} \tag{9}$$

Thus, we obtain

$$\begin{cases} \dot{\varphi} = \dfrac{v}{R_c}\operatorname{sgn}\dot{\varphi}, \\ \dot{v} = g\sin\beta\sin\varphi - v^2\dfrac{C_d\rho_a s}{2m} - \mu g\cos\beta. \end{cases} \tag{10}$$

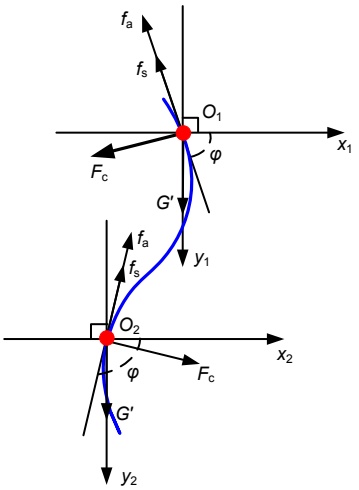

Fig. 4 Plane force analysis performed on the admissible trajectory

3.3 Dynamic equations

The trajectory equation of the particle can be described by four state variables:

$$\begin{cases} x = x(t), \\ y = y(t), \\ \varphi = \varphi(t), \\ v = v(t), \end{cases} \tag{11}$$

where $x(t)$, $y(t)$, $\varphi(t)$, and $v(t)$ are the lateral displacement, longitudinal displacement, angle between the tangent and horizontal direction, and tangential

velocity of the trajectory curve, respectively. According to the kinematics, the following equations are obtained:

$$\begin{cases}\dot{x}=v\cos\varphi,\\ \dot{y}=v\sin\varphi.\end{cases} \tag{12}$$

Combining Eqs. (10) and (12), the dynamic equation $\dot{\boldsymbol{z}}=\boldsymbol{f}(\boldsymbol{z}, u, t)$ can be expressed as follows:

$$\begin{cases}\dot{x}=v\cos\varphi,\\ \dot{y}=v\sin\varphi,\\ \dot{\varphi}=vu(t),\\ \dot{v}=g\sin\beta\sin\varphi-v^2\dfrac{C_\mathrm{d}\rho_\mathrm{a}s}{2m}-\mu g\cos\beta,\end{cases} \tag{13}$$

where the control variable $u(t)$ is defined as

$$u(t)=\frac{1}{R_\mathrm{c}(t)}\mathrm{sgn}\dot{\varphi}(t). \tag{14}$$

The control variable describes the bending degree and direction of the ski trajectory. Skiers can achieve the quickest trajectory by controlling the control variable.

3.4 Boundary conditions

The original trajectory optimization problem is converted into a multi-phase optimal control problem, and the whole ski trajectory is divided into eight phases on the Super-G course. The first phase is between the starting point and the first gate line; the second phase is between the first and the second gate lines; the third phase is between the second and the third gate lines; the remaining phases are defined in the same way. Let $t_0\{p\}$ be the initial time of the p^{th} phase and $t_0\{1\}$ the time when the skier leaves the starting point $O(0, 0)$. Similarly, let $t_\mathrm{f}\{p\}$ be the final time of the p^{th} phase and $t_\mathrm{f}\{8\}$ the time when the skier passes the finish line. Let the initial, final, and general states of the p^{th} phase be expressed, respectively, as follows:

$$\boldsymbol{z}_0^{(p)}=[x_0\{p\}, y_0\{p\}, \varphi_0\{p\}, v_0\{p\}]^\mathrm{T}, \tag{15}$$

$$\boldsymbol{z}_\mathrm{f}^{(p)}=[x_\mathrm{f}\{p\}, y_\mathrm{f}\{p\}, \varphi_\mathrm{f}\{p\}, v_\mathrm{f}\{p\}]^\mathrm{T}, \tag{16}$$

$$\boldsymbol{z}^{(p)}=[x\{p\}, y\{p\}, \varphi\{p\}, v\{p\}]^\mathrm{T}. \tag{17}$$

To obtain the optimal trajectory, time and states are constrained as

$$\begin{cases}t_0\{1\}=0\ \mathrm{s},\\ t_0\{q+1\}=t_\mathrm{f}\{q\},\\ 0\ \mathrm{s}\le t_\mathrm{f}\{p\}\le 30\ \mathrm{s},\end{cases} \tag{18}$$

$$\begin{cases}x_0\{1\}=0\ \mathrm{m},\\ x_0\{q+1\}=x_\mathrm{f}\{q\},\\ x_{p1}\le x_\mathrm{f}\{p\}\le x_{p2},\\ -20\ \mathrm{m}\le x\{p\}\le 20\ \mathrm{m},\end{cases} \tag{19}$$

$$\begin{cases}y_0\{1\}=0\ \mathrm{m},\\ y_0\{q+1\}=y_\mathrm{f}\{q\},\\ y_\mathrm{f}\{p\}=y_{p1},\\ 0\ \mathrm{m}\le y\{p\}\le 235\ \mathrm{m},\end{cases} \tag{20}$$

$$\begin{cases}\varphi_0\{1\}=\pi/2,\\ \varphi_0\{q+1\}=\varphi_\mathrm{f}\{q\},\\ 0\le\varphi_\mathrm{f}\{p\}\le\pi,\\ 0\le\varphi\{p\}\le\pi,\end{cases} \tag{21}$$

$$\begin{cases}v_0\{1\}=5\ \mathrm{m/s},\\ v_0\{q+1\}=v_\mathrm{f}\{q\},\\ 0\ \mathrm{m/s}\le v_\mathrm{f}\{p\}\le 50\ \mathrm{m/s},\\ 0\ \mathrm{m/s}\le v\{p\}\le 50\ \mathrm{m/s},\end{cases} \tag{22}$$

where q=1, 2, …, 7, p=1, 2, …, 8, x_{p1} and x_{p2} are the x-axis coordinates of P_{p1} and P_{p2} respectively, and y_{p1} is the y-axis coordinate of P_{p1}.

3.5 Objective function

In this study, the purpose of trajectory optimization is to minimize the final race time of the whole skiing process, so it is a minimum-time problem. Such a problem can be considered the minimization of the objective function:

$$J=\int_0^{t_\mathrm{f}}\mathrm{d}t=t_\mathrm{f}, \tag{23}$$

where t_f is equal to $t_\mathrm{f}\{8\}$.

3.6 Problem solving

For the solution to the trajectory optimization problem, a pseudospectral method is used. The basic principle of the pseudospectral method is to approximate the state variables and control variables using a set of basis functions that are typically Lagrange interpolation polynomials, and the differential algebraic constraint conditions are enforced at a specified set of collocation points (Tang and Chen,

2016).

According to the choice of discrete points, the pseudospectral methods include mainly the Legendre pseudospectral method (LPM), Gauss pseudospectral method (GPM), Chebychev pseudospectral method (CPM), and Radau pseudospectral method (RPM). In this study, RPM is adopted for the solution to the trajectory optimization problem, the interpolation polynomial of which is the Lagrange polynomial and the discrete point is the Legendre-Gauss-Radau (LGR) point (Garg et al., 2009; Jiang et al., 2017). Calculation steps are described as follows:

First, an affine transformation is defined as

$$t=\frac{t_\mathrm{f}-t_0}{2}\tau+\frac{t_\mathrm{f}+t_0}{2}, \tag{24}$$

where $\tau\in[-1, 1]$. The dynamic equation $\dot{\boldsymbol{z}}=\boldsymbol{f}(\boldsymbol{z}, u, t)$ can be written as

$$\frac{\mathrm{d}\boldsymbol{z}}{\mathrm{d}\tau}=\frac{t_\mathrm{f}-t_0}{2}\boldsymbol{f}(\boldsymbol{z}(\tau),u(\tau),\tau;t_0,t_\mathrm{f}). \tag{25}$$

Next, the state variable $\boldsymbol{z}(\tau)$ is approximated using Lagrange interpolation polynomials:

$$\boldsymbol{z}(\tau)\approx\sum_{i=1}^{N}\boldsymbol{z}(\tau_i)L_i(\tau), \tag{26}$$

where $\{\tau_i\}_{i=1}^N$ are the LGR collocation points (i=1:N−1) and the terminal point (i=N), τ_N=1. $\{L_i(\tau)\}_{i=1}^N$ are the bases of the Lagrange interpolation polynomials and are defined as

$$L_i(\tau)=\prod_{j=1,j\neq i}^{N}\frac{\tau-\tau_j}{\tau_i-\tau_j},\ i=1,2,\ldots,N, \tag{27}$$

from which it can be found that

$$L_i(\tau_j)=\begin{cases}1, & j=i,\\ 0, & j\neq i,\end{cases}\quad i,j=1,2,\ldots,N. \tag{28}$$

Then, time derivative of the state approximation of Eq. (26) is given as

$$\dot{\boldsymbol{z}}(\tau_k)\approx\sum_{i=1}^{N}\boldsymbol{z}(\tau_i)\dot{L}_i(\tau_k)=\sum_{i=1}^{N}D_{ki}\boldsymbol{z}(\tau_i), \tag{29}$$

where k=1, 2, …, N−1.

Finally, the dynamic constraint equation is collocated at the (N−1) LGR points as follows:

$$\sum_{i=1}^{N}D_{ki}\boldsymbol{z}(\tau_i)-\frac{t_\mathrm{f}-t_0}{2}\boldsymbol{f}(\boldsymbol{z}(\tau_k),u(\tau_k),\tau_k;t_0,t_\mathrm{f})=\boldsymbol{0}, \tag{30}$$

where $D_{ki}=\dot{L}_i(\tau_k)$ (k=1, 2, …, N−1, i=1, 2, …, N) is the element of the (N−1)×N Radau pseudospectral differentiation matrix.

Similarly, the control variable $u(\tau)$ is approximated using Lagrange interpolation polynomials:

$$u(\tau)\approx\sum_{k=1}^{N-1}u(\tau_k)L_k(\tau), \tag{31}$$

where τ_1, τ_2, …, τ_{N-1} are the interpolation nodes.

The system equations and objective function expressed using the RPM are as follows:

$$\begin{cases}\sum\limits_{i=1}^{N}D_{ki}x(\tau_i)=\dfrac{t_\mathrm{f}-t_0}{2}v(\tau_k)\cos(\varphi(\tau_k)),\\ \sum\limits_{i=1}^{N}D_{ki}y(\tau_i)=\dfrac{t_\mathrm{f}-t_0}{2}v(\tau_k)\sin(\varphi(\tau_k)),\\ \sum\limits_{i=1}^{N}D_{ki}\varphi(\tau_i)=\dfrac{t_\mathrm{f}-t_0}{2}v(\tau_k)u(\tau_k),\\ \sum\limits_{i=1}^{N}D_{ki}v(\tau_i)=\dfrac{t_\mathrm{f}-t_0}{2}\{g\sin\beta\sin(\varphi(\tau_k))\\ \qquad -[C_\mathrm{d}\rho_\mathrm{a}s/(2m)]v^2(\tau_k)-\mu g\cos\beta\},\end{cases} \tag{32}$$

$$J=\frac{t_\mathrm{f}-t_0}{2}\int_{-1}^{1}1\,\mathrm{d}\tau\approx\frac{t_\mathrm{f}-t_0}{2}\sum_{k=1}^{N-1}w_k, \tag{33}$$

where w_k (k=1, 2, …, N−1) are the LGR weights.

4 Simulation results and discussion

In this section, numerical solution is carried out using the MATLAB optimization toolbox and simulation results are given.

4.1 Optimal trajectory

Suppose the mass of the whole system m=65 kg, gravity acceleration g=9.8 m/s^2, angle of the ski slope β=20°, air resistance coefficient C_d=0.45, air density ρ_a=1.225 kg/m^3, windward area of the human body s=0.4 m^2, and sliding friction coefficient μ=0.03.

Let the control variable be constrained by

$-0.046 \le u(t) \le 0.046$ and then the optimal trajectory can be obtained.

It can be seen from Fig. 5c that there is a straight line in the fifth and eighth phases, according to the tangential angle that changes much more slowly (almost remains constant) within a certain interval of the two phases, but not over the whole skier trajectories of the two phases.

From the changes of $u(t)$ in Fig. 5e, three typical features should be noted. First, the control variable remains constant near the turning poles, which means that the skier passes through each gate with a certain turning radius generally. Second, the control variable fluctuates over a period of time at each phase. According to the definition of the control variable (Eq. (14)), it can be split into two parts: $1/R_c(t)$ and $\operatorname{sgn}\dot{\varphi}(t)$. The former can be regarded as a numerical magnitude, while the latter is related mainly to the turning direction. When the rate of the tangential angle curve changes slightly at some points, the

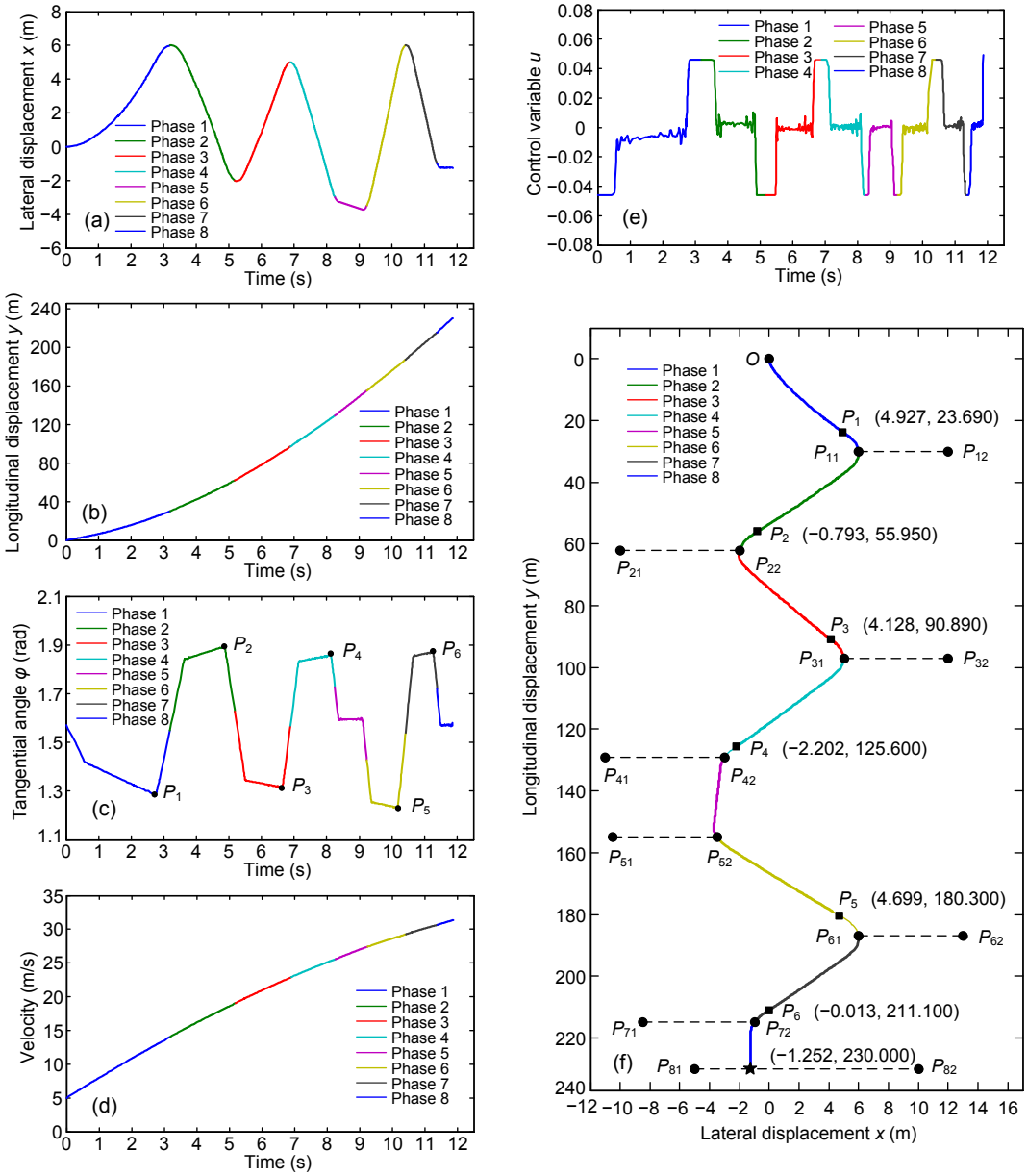

Fig. 5 Changes in the lateral (a) and longitudinal (b) displacements over time, tangential angle curve (c), velocity curve (d), control variable changing curve (e), and the optimal trajectory curve where the coordinates of the gliding inflection points are shown (f)

control variable will fluctuate correspondingly. In other words, the control variable is constrained by $\operatorname{sgn}\dot{\varphi}(t)$. Third, the change of $u(t)$ seems fast at some moments (almost like the Heaviside step function) mainly due to the function characteristic of $\operatorname{sgn}\dot{\varphi}(t)$, which jumps at $\dot{\varphi}(t)=0$ (i.e., $\dot{\varphi}(t)=0$ is a jump break point).

As shown in Fig. 5f, the optimal trajectory of the Super-G course in this study is a smooth curve that satisfies the condition of being an admissible trajectory. Calculated numerically by MATLAB, the coordinates of the gliding inflection points (P_1–P_6) can be obtained and marked on the trajectory, which are considered to be the transition points for concavity and convexity in the skier trajectory curve and can tell skiers when and where they should begin to swing around the turning poles. At the same time, the minimum time worked out is 11.86 s.

However, the final time is different because of the control variables with different upper and lower limits. In Table 1, 20 groups of data points are listed, and we refer to the minimum turning radius of 17.2 m (Gilgien et al., 2014) (the corresponding curvature value is 0.058). Based on this, the control variable is constrained to a certain range. It can be seen that the final time decreases with the increase of the control variable, which shows that the smaller the minimum turning radius, the shorter the total skiing time.

Through further simulations, Figs. 5−7 show that solutions with higher upper limits of the control variable $u(t)$ yield shorter runtimes and straighter (or shorter) paths from gate to gate, which does not contradict with the conclusions in Lind and Sanders (2004), who stated that the shortest path between two points on a slope is not necessarily the fastest path. A more important factor is the different nature of our problem. In contrast to Lind and Sanders (2004), our quickest descent path is subject to constraints requiring the path to pass through a set of gates. While Lind and Sanders (2004)'s solution allows skiers to reach the first gate quickly, the exit parameters of their trajectory are likely to make the path between the first and the second gate lines longer, which takes longer runtime than our method, unless the curvature radius is allowed to become very small at the first gate and so on.

From Figs. 6 and 7, it is found that although the total skiing time is reduced, the minimum turning radius also decreases, which is more difficult for alpine skiers to achieve. According to the relevant research on alpine skiing (Spörri et al., 2016, 2017), a high skiing speed combined with a small turning radius can shorten the skiing time, but it will increase the acting ground reaction force and cause a higher risk of sideslip and even injury. That is to say, the smaller the minimum turning radius, the higher the requirements for alpine skiers in the Super-G.

For the accuracy to 0.01 s (the precision mentioned here referring to the total skiing time obtained by numerical computation is kept to the decimal place and the time is accurate to the hundredth in alpine skiing competition), considering both skiing time and skiing safety, the trajectory shown in Fig. 5f is regarded to be optimal.

4.2 Code testing

To show that our simulation code works properly, a useful test has been carried out. We set air drag and sliding friction to zero and check that our optimization method delivers the same solution to the one-phase problem (start-to-first gate) as in Lind and Sanders (2004).

Based on the results of Lind and Sanders (2004), we can obtain the parametric equation of a cycloid as

$$\begin{cases} x = R(\phi - \sin\phi), \\ y = R(1 - \cos\phi), \end{cases} \tag{34}$$

where ϕ is a rolling angle and radius $R=A/(2g')$ (A is a constant and g' the effective gravitational acceleration for the slope).

The starting and final points are $O(0, 0)$ and $P_{11}(6, 30)$, respectively. The following equation holds:

$$\begin{cases} 6 = R_{11}(\phi_{11} - \sin\phi_{11}), \\ 30 = R_{11}(1 - \cos\phi_{11}). \end{cases} \tag{35}$$

Using MATLAB, two parameters are obtained: $\phi_{11}=0.5930$ rad and $R_{11}=175.7356$ m. The brachistochrone trajectory on the ski slope can be described as

$$\begin{cases} x = 175.7356(\phi - \sin\phi), \\ y = 175.7356(1 - \cos\phi). \end{cases} \tag{36}$$

In addition, to obtain the one-phase optimal

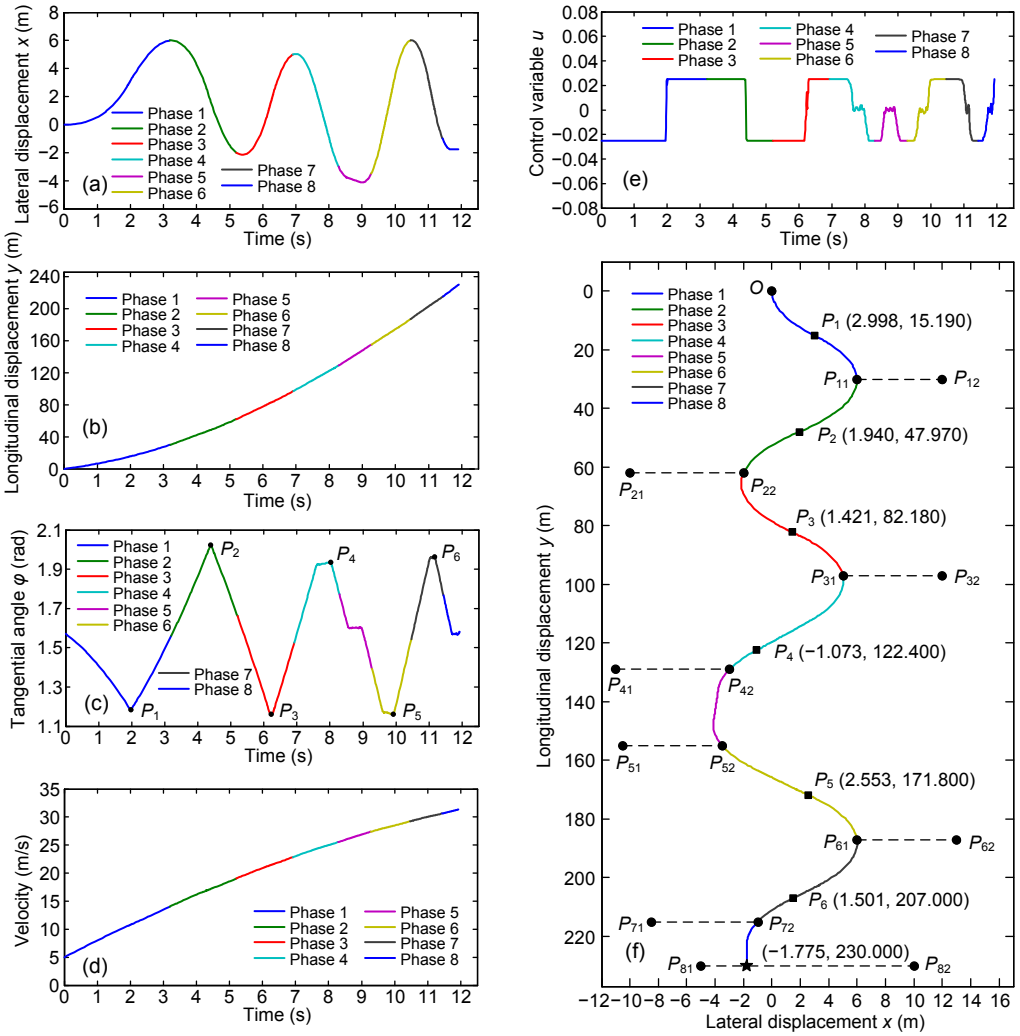

Fig. 6 Simulation results when the control variable is constrained by $-0.025 \le u(t) \le 0.025$ under the constraint conditions of Eqs. (18)–(22): (a) lateral displacements; (b) longitudinal displacements; (c) tangential angle curve; (d) velocity curve; (e) control variable changing curve; (f) the optimal trajectory curve

trajectory by our optimization method, time and states are constrained as follows:

$$\begin{cases} t_0\{1\} = 0\ \text{s}, \\ 0\ \text{s} \le t_\text{f}\{1\} \le 30\ \text{s}. \end{cases} \tag{37}$$

$$\begin{cases} x_0\{1\} = 0\ \text{m}, \\ 6\ \text{m} \le x_\text{f}\{1\} \le 12\ \text{m}, \\ -20\ \text{m} \le x\{1\} \le 20\ \text{m}, \end{cases} \tag{38}$$

$$\begin{cases} y_0\{1\} = 0\ \text{m}, \\ y_\text{f}\{1\} = 30\ \text{m}, \\ 0\ \text{m} \le y\{1\} \le 235\ \text{m}, \end{cases} \tag{39}$$

$$\begin{cases} \varphi_0\{1\} = \pi/2, \\ 0 \le \varphi_\text{f}\{1\} \le \pi, \\ 0 \le \varphi\{1\} \le \pi, \end{cases} \tag{40}$$

$$\begin{cases} v_0\{1\} = 5\ \text{m/s}, \\ 0\ \text{m/s} \le v_\text{f}\{1\} \le 50\ \text{m/s}, \\ 0\ \text{m/s} \le v\{1\} \le 50\ \text{m/s}. \end{cases} \tag{41}$$

According to Table 1, for the accuracy to 0.01 s, 0.046 is the best limit of the control variable with the shortest time 11.86 s mentioned above. Likewise, let the control variable be constrained by $-0.046 \le u(t) \le 0.046$. Test results are shown in Fig. 8.

In Fig. 8f, it can be seen that our solution is almost coincident with Lind and Sanders (2004)'s solution, both of which are parts of a cycloid. This suggests that our method delivers the same solution to the one-phase trajectory optimization problem as in Lind and Sanders (2004). Moreover, the test results

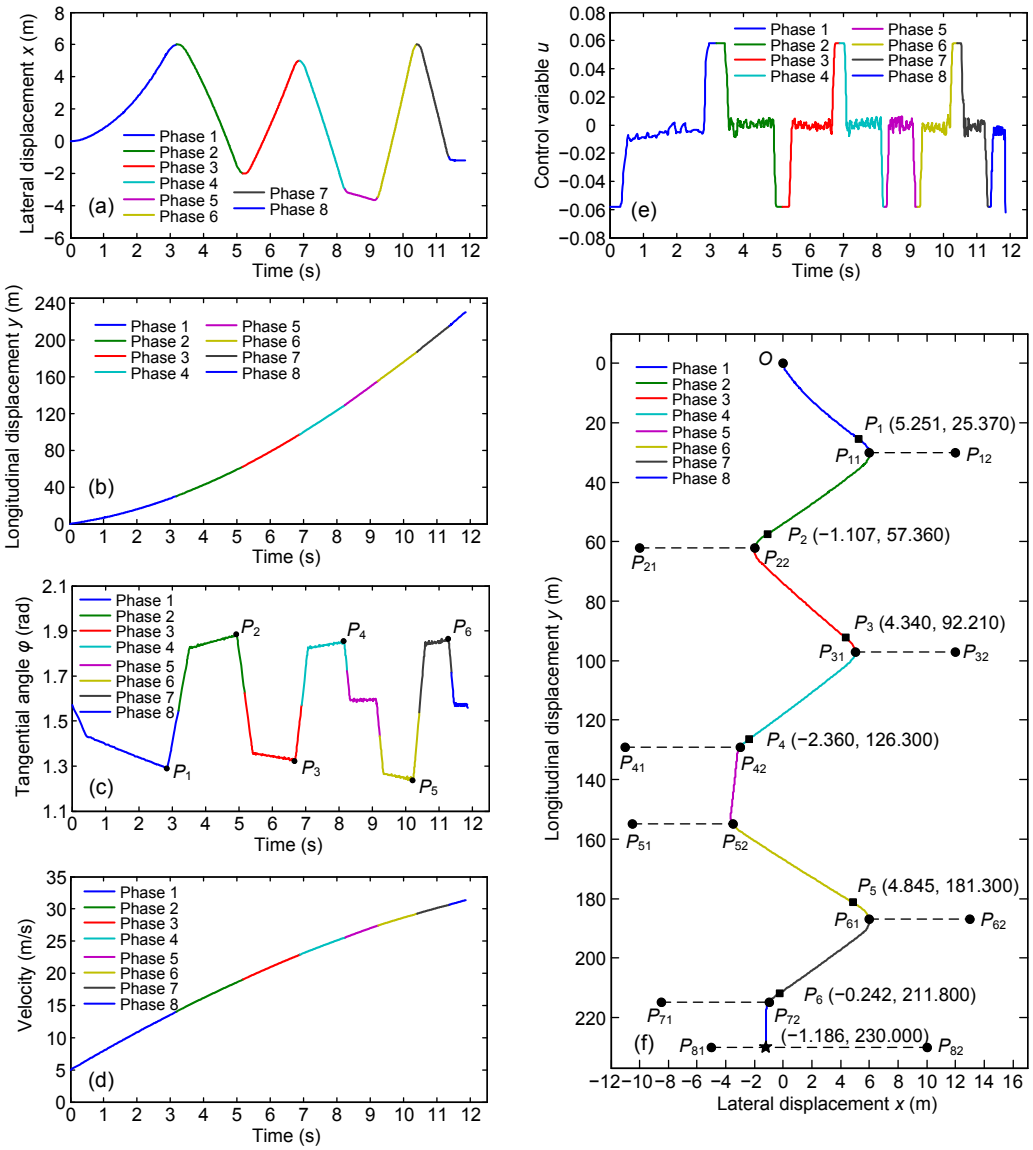

Fig. 7 Simulation results when the control variable is constrained by $-0.058 \le u(t) \le 0.058$ under the constraint conditions of Eqs. (18)–(22): (a) lateral displacements; (b) longitudinal displacements; (c) tangential angle curve; (d) velocity curve; (e) control variable changing curve; (f) the optimal trajectory curve

Table 1 Minimum time for the optimal trajectories with different upper and lower limits of control variables

Upper and lower limits of $u(t)$	Convergence/ Divergence	Final time (s)	Upper and lower limits of $u(t)$	Convergence/ Divergence	Final time (s)
±0.019	d	–	±0.040	c	11.8712
±0.021	d	–	±0.042	c	11.8687
±0.023	d	–	±0.044	c	11.8666
±0.025	c	11.9195	±0.046	c	11.8647
±0.030	c	11.8919	±0.048	c	11.8631
±0.031	c	11.8887	±0.050	c	11.8616
±0.033	c	11.8834	±0.052	c	11.8602
±0.035	c	11.8791	±0.054	c	11.8590
±0.037	c	11.8755	±0.056	c	11.8579
±0.039	c	11.8725	±0.058	c	11.8569

Skiing time listed is accurate to four decimal places for comparison. "–" means that the numerical results cannot be worked out

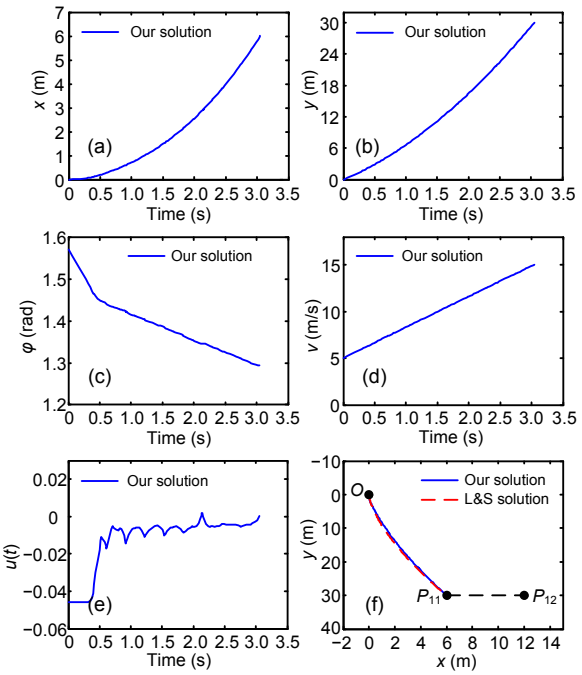

Fig. 8 Code testing results for the one-phase trajectory optimization problem (start-to-first gate) under the constraint conditions of Eqs. (37)–(41): (a) lateral displacements; (b) longitudinal displacements; (c) tangential angle curve; (d) velocity curve; (e) control variable changing curve; (f) the optimal trajectory curve

not only show that our multi-phase trajectory optimization problem is obviously different from the one-phase problem in nature, but also verify that our code is well designed and is effective.

5 Conclusions and future work

In this study, we established a trajectory optimization model for alpine skiers in the Super-G and demonstrated its rationality and validity by numerical simulations. In contrast to the previous achievements in alpine skiing, we have obtained the optimal trajectory of a specific Super-G course to provide alpine skiers with help and reference. Based on this, we have made parameter optimization and carried out a useful test for our code. Results showed that the skier trajectory can be considered optimal within a reasonable range of control variables after comprehensive consideration of safety and time. Furthermore, we have marked the inflection points on the skier trajectory, and obtained the coordinates by working out the transition points for concavity and convexity in the skiing curve. The concept and coordinate labeling of the inflection points on the optimal trajectory have not been presented in other papers.

Several skiing suggestions for alpine skiers have been presented. At first, choose the optimal route. Alpine skiers should ski along an S-shape trajectory and be as close as possible to the turning poles when passing through the gates in a correct way. Then, turn at the inflection points. Generally speaking, inflection points are closer to the turning poles (Fig. 5f), and their positions are different for different gates or different courses. However, the positions of the inflection points are too far from the turning poles; i.e., skiers begin a turn far from the turning poles when passing through the gates (Fig. 6f). Finally, ski with a small turning radius. Considering the risks of alpine skiing, it is recommended that skiers should reduce the turning radius to achieve a faster skiing trajectory on the premise of ensuring safety and not breaking the rules.

In addition to establishing the trajectory optimization model, simulation results have been analyzed and the optimal trajectory has been obtained, although some details were ignored in the modeling process, such as geometric features of the skis and postural angles of the human body. Therefore, we will carry out in-depth research and analysis to improve the model in future work.

Contributors

Cong-ying CAI and Xiao-lan YAO designed the research. Cong-ying CAI processed the data and drafted the manuscript. Xiao-lan YAO helped organize the manuscript. Cong-ying CAI and Xiao-lan YAO revised and finalized the paper.

Compliance with ethics guidelines

Cong-ying CAI and Xiao-lan YAO declare that they have no conflict of interest.

References

Benito J, Johnson BJ, 2016. Trajectory optimization for a Mars ascent vehicle. AIAA/AAS Astrodynamics Specialist Conf, Article 5441. https://doi.org/10.2514/6.2016-5441

Betts JT, 1998. Survey of numerical methods for trajectory optimization. *J Guid Contr Dynam*, 21(2):193-207. https://doi.org/10.2514/2.4231

Chen D, Li SQ, Wang JF, et al., 2019. A multi-objective trajectory planning method based on the improved immune clonal selection algorithm. *Manufacturing*, 59:431-442. https://doi.org/10.1016/j.rcim.2019.04.016

Chen G, Fu Y, Guo JF, 2011. Survey of aircraft trajectory optimization methods. *Flight Dynam*, 29(4):1-5 (in

Chinese). https://doi.org/10.13645/j.cnki.f.d.2011.04.008

Chen L, Qi ZH, 2006. Analyses of mechanical characteristics for alpine ski. *J Dalian Univ Technol*, 46(6):781-784 (in Chinese). https://doi.org/10.3321/j.issn:1000-8608.2006.06.001

Crain A, Ulrich S, 2019. Experimental validation of pseudospectral-based optimal trajectory planning for free-floating robots. *J Guid Contr Dynam*, 42(8):1726-1742. https://doi.org/10.2514/1.G003528

Dębski R, 2014. High-performance simulation-based algorithms for an alpine ski racer's trajectory optimization in heterogeneous computer systems. *Int J Appl Math Comput Sci*, 24(3):551-566. https://doi.org/10.2478/amcs-2014-0040

Dębski R, 2016. An adaptive multi-spline refinement algorithm in simulation based sailboat trajectory optimization using onboard multi-core computer systems. *Int J Appl Math Comput Sci*, 26(2):351-365. https://doi.org/10.1515/amcs-2016-0025

Falck RD, Gray JS, 2019. Optimal control within the context of multidisciplinary design, analysis, and optimization. AIAA Scitech Forum, Article 0976. https://doi.org/10.2514/6.2019-0976

Garg D, Patterson MA, Darby CL, et al., 2009. Direct trajectory optimization and costate estimation of general optimal control problems using a Radau pseudospectral method. AIAA Guidance, Navigation, and Control Conf, Article 5989. https://doi.org/10.2514/6.2009-5989

Gilgien M, Spörri J, Kröll J, et al., 2014. Mechanics of turning and jumping and skier speed are associated with injury risk in men's World Cup alpine skiing: a comparison between the competition disciplines. *Br J Sport Med*, 48(9):742-747. https://doi.org/10.1136/bjsports-2013-092994

Graham KF, Rao AV, 2015. Minimum-time trajectory optimization of multiple revolution low-thrust Earth-orbit transfers. *J Spacecr Rockets*, 52(3):711-727. https://doi.org/10.2514/1.A33187

Guo Y, Ma JQ, Xiong CF, et al., 2019. Joint optimization of vehicle trajectories and intersection controllers with connected automated vehicles: combined dynamic programming and shooting heuristic approach. *Trans Res Part C Emerg Technol*, 98:54-72. https://doi.org/10.1016/j.trc.2018.11.010

Hirano Y, 2006. Quickest descent line during alpine ski racing. *Sport Eng*, 9(4):221-228. https://doi.org/10.1007/BF02866060

Hong SM, Seo MG, Shim SW, et al., 2016. Sensitivity analysis on weight and trajectory optimization results for multi-stage guided missile. *IFAC-PapersOnLine*, 49(17):23-27. https://doi.org/10.1016/j.ifacol.2016.09.005

Huang GQ, Lu YP, Nan Y, 2012. A survey of numerical algorithms for trajectory optimization of flight vehicles. *Sci China Technol Sci*, 55(9):2538-2560. https://doi.org/10.1007/s11431-012-4946-y

Jiang RY, Chao T, Wang SY, et al., 2017. Low-thrust trajectory in interplanetary flight solved by pseudospectral method. *J Syst Simul*, 29(2):2043-2052, 2058 (in Chinese). https://doi.org/10.16182/j.issn1004731x.joss.201709022

Komissarov S, 2019. Dynamics of carving runs in alpine skiing. I. The basic centrifugal pendulum. https://doi.org/10.31236/osf.io/gp3ef

Li TC, 2019. Single-road-constrained positioning based on deterministic trajectory geometry. *IEEE Commun Lett*, 23(1):80-83. https://doi.org/10.1109/LCOMM.2018.2879478

Li TC, Chen HM, Sun SD, et al., 2019. Joint smoothing and tracking based on continuous-time target trajectory function fitting. *IEEE Trans Autom Sci Eng*, 16(3):1476-1483. https://doi.org/10.1109/TASE.2018.2882641

Lind DA, Sanders SP, 2004. The brachistochrone problem: the path of quickest descent. In: Lind DA, Sanders SP (Eds.), The Physics of Skiing. Springer, New York, NY. https://doi.org/10.1007/978-1-4757-4345-6_19

Liu WS, Liang XL, Ma YZ, et al., 2019. Aircraft trajectory optimization for collision avoidance using stochastic optimal control. *Asian J Contr*, 21(5):2308-2320. https://doi.org/10.1002/asjc.1855

Morbidi F, Bicego D, Ryll M, et al., 2018. Energy-efficient trajectory generation for a hexarotor with dual-tilting propellers. IEEE/RSJ Int Conf on Intelligent Robots and Systems, p.6226-6232. https://doi.org/10.1109/IROS.2018.8594419

Paek SW, de Weck O, Polany R, et al., 2016. Asteroid deflection campaign design integrating epistemic uncertainties. Proc IEEE Aerospace Conf, p.1-14. https://doi.org/10.1109/AERO.2016.7500905

Patrón RSF, Botez RM, 2015. Flight trajectory optimization through genetic algorithms for lateral and vertical integrated navigation. *J Aerosp Inform Syst*, 12(8):533-544. https://doi.org/10.2514/1.I010348

Ranogajec V, Ivanović V, Deur J, et al., 2018. Optimization-based assessment of automatic transmission double-transition shift controls. *Contr Eng Pract*, 76:155-166. https://doi.org/10.1016/j.conengprac.2018.04.016

Rao AV, 2014. Trajectory optimization: a survey. In: Waschl H, Kolmanovsky I, Steinbuch M, et al. (Eds.), Optimization and Optimal Control in Automotive Systems. Springer, Cham, p.3-21. https://doi.org/10.1007/978-3-319-05371-4_1

Rudakov R, Lisovski A, Ilyalov O, et al., 2010. Optimisation of the skiers trajectory in special slalom. *Proc Eng*, 2(2):3179-3182. https://doi.org/10.1016/j.proeng.2010.04.129

Spörri J, Kröll J, Gilgien M, et al., 2016. Sidecut radius and the mechanics of turning—equipment designed to reduce risk of severe traumatic knee injuries in alpine giant slalom ski racing. *Br J Sport Med*, 50(1):14-19. https://doi.org/10.1136/bjsports-2015-095737

Spörri J, Kröll J, Gilgien M, et al., 2017. How to prevent injuries in alpine ski racing: what do we know and where do we go from here? *Sport Med*, 47(4):599-614.

https://doi.org/10.1007/s40279-016-0601-2

Sundström D, Carlsson P, Tinnsten M, 2011. Optimizing pacing strategies on a hilly track in cross-country skiing. *Proc Eng*, 13:10-16. https://doi.org/10.1016/j.proeng.2011.05.044

Tang XJ, Chen J, 2016. Direct trajectory optimization and costate estimation of infinite-horizon optimal control problems using collocation at the flipped Legendre-Gauss-Radau points. *IEEE/CAA J Autom Sin*, 3(2):174-183. https://doi.org/10.1109/JAS.2016.7451105

von Stryk O, Bulirsch R, 1992. Direct and indirect methods for trajectory optimization. *Ann Oper Res*, 37(1):357-373. https://doi.org/10.1007/BF02071065

Wang JB, Cui NG, Wei CZ, 2019. Optimal rocket landing guidance using convex optimization and model predictive control. *J Guid Contr Dynam*, 42(5):1078-1092. https://doi.org/10.2514/1.G003518

Youn SH, 2018. Can a skier make a circular turn without any active movement? *J Korean Phys Soc*, 73(10):1410-1419. https://doi.org/10.3938/jkps.73.1410

Zhang S, Hou MS, 2016. Trajectory optimization of aerocraft based on shaping and dimension reduction. *Acta Armament*, 37(6):1125-1130 (in Chinese). https://doi.org/10.3969/j.issn.1000-1093.2016.06.022

Zheng DK, Wang SY, Meng QW, 2016. Dynamic programming track-before-detect algorithm for radar target detection based on polynomial time series prediction. *IET Radar Sonar Nav*, 10(8):1327-1336. https://doi.org/10.1049/iet-rsn.2015.0332